Environment International 126 (2019) 717–726

Contents lists available at ScienceDirect

Environment International

journal homepage: www.elsevier.com/locate/envint

Distribution and speciation of copper in rice (*Oryza sativa* L.) from mining-impacted paddy soil: Implications for copper uptake mechanisms

Jin-li Cui[a,b], Yan-ping Zhao[a], Ying-Jui Lu[c], Ting-shan Chan[c], Li-li Zhang[d], Daniel C.W. Tsang[a], Xiang-dong Li[a,*]

[a] Department of Civil and Environmental Engineering, The Hong Kong Polytechnic University, Hung Hom, Kowloon, Hong Kong
[b] Key Laboratory for Water Quality and Conservation of the Pearl River Delta, Ministry of Education, School of Environmental Science and Engineering, Guangzhou University, Guangzhou, China
[c] National Synchrotron Radiation Research Center, 101 Hsin-Ann Road, Hsinchu Science Park, Hsinchu 30076, Taiwan
[d] Shanghai Synchrotron Radiation Facility, Shanghai Advanced Research Institute, Chinese Academy of Sciences, Shanghai 201204, China

ARTICLE INFO

Keywords:
Speciation and mobilization
Paddy soil
Heavy metal remediation
Tolerance and detoxification
Synchrotron-based X-ray absorption spectroscopy

ABSTRACT

Long term mining activities can cause significant metal pollution in the environment, thereby showing potential risk to the paddy field. Elucidating the interfacial processes of trace metals from contaminated paddy soil to rice within the rhizosphere can provide important information on metal biogeochemistry and food safety. The current study aims to explore the spatial distribution and molecular speciation of Cu from rhizosphere to rice plant in a mining-impacted paddy soil, and reveal the possible uptake mechanisms. X-ray absorption near edge structure (XANES) analysis indicated that Cu was primarily associated with iron oxide and sulfide in soil with a minor proportion of organic complexed species. In the rice samples, Cu showed much higher concentrations in the roots than the shoots, as most Cu was sequestered in the root surface and epidermis (primarily in the form of C/N ligands bound Cu species), rather than root xylem, as identified by micro X-ray fluorescence (μ-XRF) imaging coupling with μ-XANES. By contrast, in the root xylem, thiol-S bound Cu(I) complex was observed, representing the reduced product of Cu(II) by thiol-S ligands in rice root. The absorbed Cu was probably transported from the root to the aerial part as C/N ligand bound Cu complex such as Cu-histidine like species, which was observed in the root xylem. The large retention capacity and reduction of Cu(II) in rice root alleviated Cu toxicity to rice, which was beneficial for food safety (e.g., lower concentration of Cu in rice grains). These findings showed for the first time that the uptake mechanisms by rice from field contaminated sites, which shed light on Cu detoxification process and potential remediation strategies.

1. Introduction

Rice is a staple ingredient for more than half the world's population. However, due to industrial and urban development worldwide, substantial paddy soil is contaminated with many trace metals from various human activities (Tóth et al., 2016; Zhou et al., 2015). High concentrations of trace metals, including Cu, Zn, and Pb, may pose significant influences on the quality of rice, and consequently affect human health (Adrees et al., 2015; Lu et al., 2015; Zhuang et al., 2009). Among trace metals, the redox-active element Cu is an essential nutrient for plant growth, however, high concentration of Cu in soil shows highly toxic effect to plant, such as growth inhibition and oxidative damage by generating reactive oxygen radicals (Adrees et al., 2015; Thounaojam et al., 2012; Wu et al., 2010; Yruela, 2009). On the other hand, the frequent flooding of paddy soil strongly affected the oxidation and reduction reactions of trace elements including Fe, S, and Cu, which reactions subsequently influence Cu speciation and mobility, and uptake by rice (Pan et al., 2016; Rinklebe et al., 2016; Sun et al., 2017; Tao et al., 2003). Therefore, it is necessary to fully understand the uptake, transformation, and toxicity/detoxification of Cu in rice grown in contaminated paddy fields.

The molecular species of Cu from soil to root in the rhizosphere can greatly affect the plant uptake processes (Shi et al., 2018). It has been reported that Cu(II) was often bound with strong thiol-S containing ligands or O/N ligands in cell wall as a part of detoxification process (Cobbett and Goldsbrough, 2002; Manceau et al., 2013; Mijovilovich et al., 2009). Two previous studies have observed Cu(I) in plant roots, including tomato and oat (Ryan et al., 2013), and rice (Lu et al., 2017),

* Corresponding author.
E-mail address: cexdli@polyu.edu.hk (X.-d. Li).

https://doi.org/10.1016/j.envint.2019.02.045
Received 2 December 2018; Received in revised form 11 February 2019; Accepted 17 February 2019
Available online 14 March 2019

suggesting the occurrence of Cu(II) reduction to Cu(I) during the uptake process by plant. Reduction of Cu(II) probably occurred at the root cell during the uptake by rice as evidenced by the lighter Cu isotopes (Jouvin et al., 2012). However, a recent study indicated that Cu(II) may be absorbed by bamboo (strategy II plant) root before reduction as only Cu(II) was observed in root (Collin et al., 2014), consistent with no lighter isotopes of Cu observed in oat root (Ryan et al., 2013). For a spatial distribution analysis, most of the uptake Cu was retained as a layer around the root rhizodermis of bamboo (Collin et al., 2014) and *Elsholtzia splendens* (Xu et al., 2015). Yet for other studies, Cu was mostly concentrated in the vascular tissues of *Oryza sativa* (Lu et al., 2017) and *Commelina communis* (Shi et al., 2011). However, most studies focused on the uptake mechanism of aqueous Cu in pot or hydroponic experiments (Collin et al., 2014; Lu et al., 2017; Ryan et al., 2013; Zhao et al., 2018). Currently, no results from previous studies indicated the location of Cu(I/II) on rice root from a transversal view and its exact binding ligand in root cross location, which is critical for understanding the Cu uptake/reduction processes from soil to plant.

The biogeochemical behaviour of Cu in plant from field contaminated soil often shows significant difference from the laboratory hydroponic experiments. The main contrast between the two scenarios is that heavy metals in field soils are not in very high concentrations of bioavailable fractions for plant uptake under long-time environmental aging processes in real soils (Martinez and Motto, 2000; McBride and Cai, 2016; Pan et al., 2016). However, the less-bioavailable fractions of trace metals in field soils may be mobilized and become bioavailable for plant due to the change of soil geochemical parameters, including pH, redox potential, (in)organic fertilizers, nutrients, metal species, and microbes in comparison with aqueous Cu(II) performed in the lab (Guo and Cutright, 2015; Rinklebe et al., 2016; Wu et al., 2010; Yang et al., 2014), which make metal biogeochemistry in field contaminated sites more complicated (Adamo et al., 2018; Hansel et al., 2001; Tao et al., 2003; Zhao et al., 2014b). Despite the evidences from previous studies, the mechanism of Cu uptake process around the root surface/epidermis from soil is still largely unknown, because of the complexity of spatial distribution of Cu molecular species on root transversal section. The in situ characterization of the oxidation state and spatial distribution of Cu within plant root and the surrounding soil are reported using synchrotron X-ray techniques in recent studies (Kopittke et al., 2017; Sun et al., 2017; Zhao et al., 2018). Therefore, the present research aims to study the critical rhizosphere zone from the contaminated field sites, focusing on the distribution, speciation, and mobility of Cu from soil to plant.

By investigating rice and their rhizosphere soils from a paddy site contaminated by long term mining activities, the current study aims to elucidate how rice absorb and transform Cu during the plant uptake process. Synchrotron based μ-XRF and μ-XANES were employed to investigate the spatial distribution and molecular speciation of Cu in the rhizosphere, especially for the rice root. To our knowledge, this research is the first investigation into the molecular fate of Cu in the interface of soil-plant system under field relevant geochemical conditions. The results may shed lights on Cu uptake and transformation mechanisms in rice, and subsequent impact on food safety assessment.

2. Materials and methods

2.1. Sample collection and treatment

Plant and corresponding rhizosphere soil samples were collected from a paddy field in Xinjiang town, which was contaminated by the Dabaoshan mining wastewater. The mining impacted site is located in Shaoguan, Guangdong province, southern China. Rhizosphere soil near plant root was carefully collected in the field. The samples were transported on ice in a cooler, and stored at 4 °C once arriving at the laboratory. Then the soil samples were air-dried in the lab, and passed through a 2-mm sieve before use. Plant samples were washed with tap water and deionized water (DIW) three times to remove the extraneous soil particles, dried at 80 °C for 3 days, and grounded before analysis. Some fresh soil and plant samples were stored at 4 °C for further synchrotron analysis.

2.2. Mobility and phytoavailability of Cu and major metals

Water available metals in soil were determined by mixing 0.01 M $CaCl_2$ with air-dried (2-mm) soil (1/10, g/mL) for 120 min. Furthermore, a rhizosphere-based extraction method was employed to investigate the phytoavailability of Cu in the soil using 10 mM combined organic acid of acetic, lactic, citric, malic, and formic acid at a molar ratio of 4:2:1:1:1 (Beiyuan et al., 2017; Feng et al., 2005). The mixture (1/10, g/mL) was shaken by an end-over-end shaker in the dark for 16 h, centrifuged, filtered, and analyzed.

2.3. Synchrotron based μ-XRF and XANES analysis

For μ-XRF and μ-XANES analysis, fresh plant root were cut into cross-sections in ~50-μm prepared according to our previous research (Cui et al., 2019). Synchrotron based μ-XRF and XANES analysis of the cross-section was performed at beamline BL15U1 at the Shanghai Synchrotron Radiation Facility (SSRF), China (Cui et al., 2013), with details shown in the supplementary information. Four points of interest (POI) in μ-XRF mapping region were selected for Cu K-edge μ-XANES analysis.

For bulk XANES analysis, fresh rice root samples were collected, washed using tap water and then DIW for three times each to remove any soil particles, ground under liquid nitrogen, and freeze-dried. All the soil and plant samples were stored at 4 °C before XANES analysis. Bulk XANES of Cu K-edge (8979 eV) and Fe K-edge (7112 eV) was performed at beamline 01C1 and beamline BL16A1, respectively, at the National Synchrotron Radiation Research Center (NSRRC) in Taiwan. Preparation of Cu and Fe standard references, principal component analysis (PCA), target transformation (TT) test, and linear combination fit (LCF) were performed as previous studies (Cui et al., 2018; Sun et al., 2017; Zhao et al., 2018). Of the standard references, Cu-oxalate represents soil organic substance bound Cu complex, Cu-alginate and Cu-histidine represent C/N ligand bound Cu complexes (Collin et al., 2014; Manceau et al., 2013; Zhao et al., 2018), which contribute to Cu sequestration by cell wall polysaccharides and amino ligands. Thiol-S ligands bound Cu(I) in plant samples were fitted using Cu(I)-glutathione or Cu(I)-cysteine, and inclusion of CuS represents sulfide bound Cu species in soil (Ryan et al., 2013; Sun et al., 2017; Yang et al., 2014). More detailed information can be found in the supplementary information (Tables S1–7).

2.4. Sample chemical analysis

The total organic carbon (TOC) of soil was determined using a TOC auto-analyzer (Shimadzu) after reaction with HCl to eliminate the inorganic carbon (carbonates). Particle-size distributions were conducted for soil texture fraction analysis using laser diffraction MS 2000 (Malvern Instrument). The percentages of the following three size ranges were determined as follows: < 0.005 mm (clay), 0.005–0.074 mm (silt), and > 0.074 mm (sand) (ASTM Committee, 1998). Analysis of soil pH, water-soluble TOC concentrations in soil, digestion of soil and plant samples, and metal analysis were reported in our previous studies (Cui et al., 2019; Li et al., 2001). Generally, pH was determined by stirring air-dried < 10-mesh-sieved soil in DIW (1/2.5, g/mL) for 30 min. Available TOC in soil were determined in the filtrated (0.45-μm) extract from reacting 4 °C stored soils with $CaCl_2$ (0.01 M) solution (1/10, g/mL) for 120 min. Soil and plant samples were digested using a pseudo-total digestion method (Li et al., 2001), analyzed using ICP-OES (Agilent, 700 Series) and ICP-MS (Agilent, 7700 Series), and reported on dry weight basis. Statistical spearman's correlation

Table 1
Soil organic contents, texture fraction, pH of soil extract by DIW, water-soluble TOC values in $CaCl_2$ extract, available Cu and Fe in soil in $CaCl_2$ extract and rhizosphere (Rhi)-based extract for the collected soil samples (series of LQ and LX and K), total concentrations of Cu and Fe in rice roots and shoots. LX4 rhi and LX4 non-rhi represent rhizosphere soil and non-rhizosphere soil collected at LX4 location.

Sample	pH	TOC (%)	Soil fraction (%) (Sand/silt/clay)	Total conc. in soil		$CaCl_2$ extract (mg/L)			Rhi-based extract (mg/L)		Total conc. in root		Total conc. in shoot	
				Cu (mg/kg)	Fe (mg/kg)	TOC	Cu	Fe	Cu	Fe	Cu (mg/kg)	Fe (mg/kg)	Cu (mg/kg)	Fe (mg/kg)
LQ1	5.45	1.80	50/42/8	734	112,000	17	0.01	0.27	1.35	43	235	73,000	14	707
LQ2	4.96	1.60	53/39/8	724	128,000	12	0.08	0.72	2.22	31	384	60,000	13	537
LQ3	4.77	1.99	54/39/7	673	108,000	17	0.19	1.76	2.59	33	396	43,000	13	638
LQ4	5.21	1.94	50/41/9	712	115,000	21	0.01	0.68	1.6	49	303	74,000	12	699
LQ5	4.72	1.55	52/41/7	597	121,000	14	0.25	1.97	3.06	37	143	73,000	24	1018
LQ6	5.07	1.85	53/39/8	514	114,000	23	0.03	3.09	1.54	60	610	83,000	11	439
LQ7	6.83	1.74	46/47/8	147	82,000	16	ND*	0.01	0.04	58	78	51,000	12	250
LQ8	4.91	1.93	49/41/10	122	76,000	29	0.02	4.13	0.31	61	96	49,000	10	251
LX1	5.79	2.08	41/49/10	797	139,000	25	ND	0.03	0.14	46	93	68,000	4	286
LX2	5.95	1.90	48/45/7	540	131,000	29	ND	0.24	0.12	61	44	71,000	10	911
LX3	5.69	2.18	47/45/7	430	112,000	29	ND	0.33	0.45	50	65	55,000	7	494
LX4 rhi	6.18	1.20	42/48/10	339	74,000	12	0.01	0.02	0.43	17	116	18,000	150	74
LX4 non-rhi	6.28	1.38	37/52/12	366	91,000	11	0.02	0.03	0.45	21	116	18,000	150	74
K	6.28	1.28	37/52/12	148	32,000	9	0.02	0.16	0.43	46	72	19,000	37	32
Median	5.57	1.82	37/39/7	527	112,000	17	0.02	0.30	0.45	46	116	58,000	12	466
Min	4.72	1.20	37/39/7	122	32,000	9	0.01	0.01	0.04	17	44	18,000	4	32
Max	6.83	2.18	54/52/12	797	139,000	29	0.25	4.13	3.06	61	610	83,000	150	1018

ND*: Not detected.

analysis was employed to evaluate the relationship among the soil geochemistry, and (available) metal concentrations in soils and plants performed using SPSS software version 22.0.

2.5. Quality assurance/quality control

Standard reference materials were used to confirm sample digestion and analysis including NIST SRM 2711a (soil) and 1573a (plant). Recovery of Cu and Fe were around 91–120% for the standard reference materials. The accuracy and precision were tested using reagent blank and analytical triplicates (standard error $<$ 10%), comprised of 10% of the total samples.

3. Results

3.1. Characterization of the paddy soil samples

Soil physico-chemical properties (pH, organic content, and soil fraction), water-soluble TOC and plant available concentrations of Cu and Fe in soil and the corresponding rice samples are shown in Table 1. Soil pH after DIW extraction ranged from 4.77 to 6.83 (Table 1). The pH was slightly lower than the recommended pH range of 6.5–7.5 for agriculture activities based on Chinese Environmental Quality Standard. Soil texture fraction exhibited three major minerals including sand with 37–54%, silt with 39–52%, and clay with 7–12%. Soil organic content showed a range of 1.20–2.18% (Table 1). After $CaCl_2$ extraction, water-soluble TOC values showed 9.3–12.2 mg/L in the extract, contributing 0.70–1.53% to total organic content of the soil. The soil texture and organic content were generally consistent with the reported soil characteristics in Guangdong province, southern China, with slightly less clay content (Tables 1 & S8) (Cai et al., 2007; Zeng et al., 2008; Zhang et al., 2018; Zhuang et al., 2009).

3.2. Copper and Fe concentrations in soil, rice root and shoot

The paddy site was severely contaminated with heavy metals from the mining activities with 122–797 mg/kg Cu (Table 1). The concentrations of Cu were 7–47 times higher than the background level (17.0 mg/kg) in Guangdong (Cui et al., 2017). $CaCl_2$ extraction showed a range of no detection (ND) to 0.25 mg/L of water available Cu in the soil (Table 1). The rhizosphere-based extraction using combined organic acids, which could reflect the plant bioavailable fraction of heavy metals more accurately (Feng et al., 2005), exhibited 0.04–3.06 mg/L, i.e., much higher than the $CaCl_2$ extraction data. For rice samples, Cu showed high concentrations of 44–610 mg/kg in root and 4–150 mg/kg in shoot (Table 1).

The concentrations of Fe in soil were analyzed with high levels of 32,000–139,000 mg/kg shown in Table 1. Accordingly, much higher available concentration of Fe was observed in the organic rhizosphere-based extract (17–61 mg/L) than that in $CaCl_2$ extract (0.01–4.13 mg/L), suggesting the facilitated dissolution of Fe oxides by naturally present organic ligands in the agricultural soil. The uptake Fe in plant reached 18,000–83,000 mg/kg in root and 30–1010 mg/kg in shoot, in agreement with previous reports of rice root containing much high concentration of Fe (Hansel et al., 2001).

3.3. Bulk XANES analysis of Cu and Fe in soil and rice root

Molecular species of Cu and Fe in soil and root samples were analyzed using bulk XANES analysis, together with the analyzed standard references shown in Figs. 1–2. The spectral features of Cu K-edge XANES standards (Fig. 1-I) were much more sensitive to the molecular coordination of Cu element in the environment, such as the main peak at region (a) representing Cu(II) species (Kau et al., 1987) and the pre-edge peaks at region (b) (8982 eV for Cu(I)-glutathione and Cu(I)-cysteine, and 8985 eV for Cu(I)Cl, respectively) for Cu(I) species (Collin et al., 2014). The related Cu references for the soil and plant samples were recorded from previous publications (Sun et al., 2017; Zhao et al., 2018), and tested for their suitability using PCA/TT and LCF analysis before fitting the sample spectra.

Copper species in the soil samples are shown in Fig. 1-II. The primary peak at ~8976 eV (region a) of the XANES spectra indicates the dominance of Cu(II) in soil. Several samples including LX1–3 also showed small pre-edge peaks at ~8985 eV, suggesting the possible occurrence of Cu(I) in paddy soil. To identify the possible Cu species in the soil samples, PCA/TT and LCF were performed on Cu K-edge XANES spectra (Cui et al., 2015a; Zhao et al., 2018). The PCA results of the eleven soil samples (Table S1) suggested four principal components with a minimum indicator (IND) value of 0.00842 contributing to 96.6% of the data set. Based on the TT results (Table S2), all the SPOIL

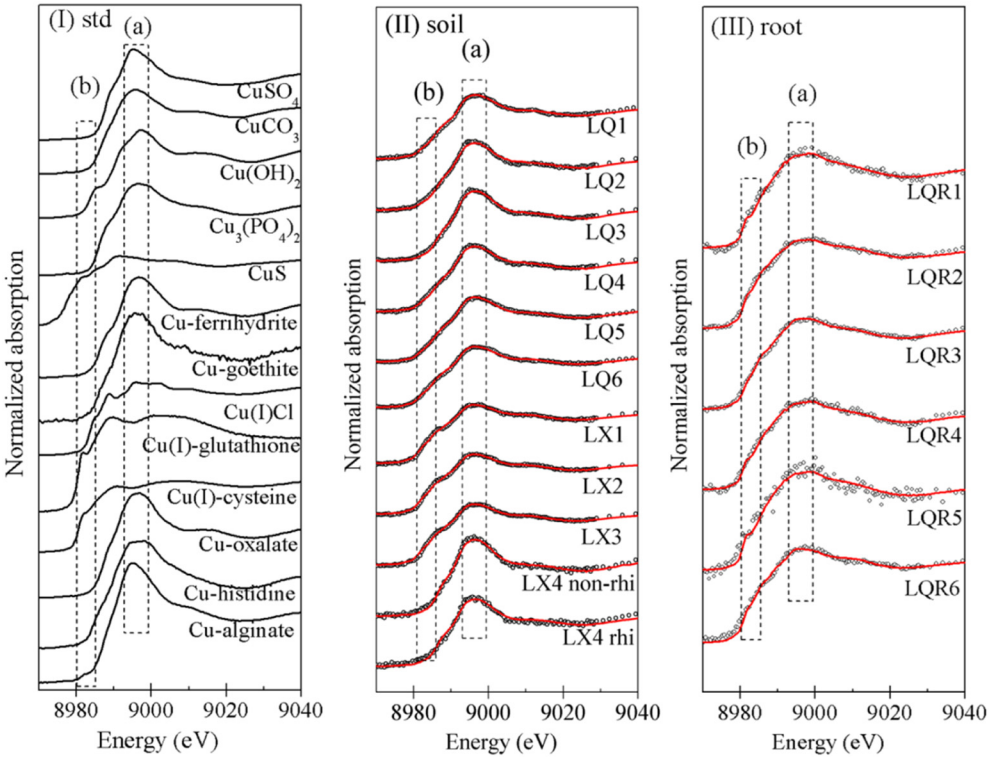

Fig. 1. Copper K-edge XANES analysis for the standard references (I), the collected soil samples (II), and root samples (III) using bulk-XANES. The XANES data were shown as black circles with linear combination fitting (LCF) as red lines. The vertical region (a) is typical peaks for Cu(II) and region (b) is pre-edge of Cu(I) characterized by Cu(I)-glutathione. The linear combination fitting results were shown in Table 2. (For interpretation of the references to color in this figure legend, the reader is referred to the web version of this article.)

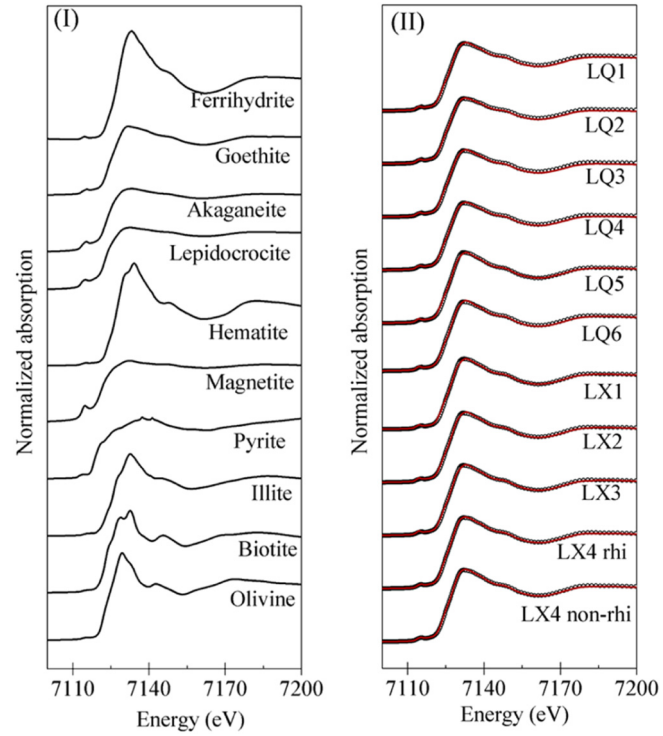

Fig. 2. Iron K-edge XANES analysis for the standard references (I) and soil samples (II). The XANES data were shown as black circles with linear combination fitting (LCF) as red lines. The linear combination fitting results were shown in Table S7. (For interpretation of the references to color in this figure legend, the reader is referred to the web version of this article.)

values were lower than three except for $Cu(OH)_2$ with SOIL value at 3.8, which is fairly acceptable according to the recommendation. Nevertheless, $Cu(OH)_2$ was excluded from LCF because of relatively low pH values of the soil samples which do not favor $Cu(OH)_2$ formation.

The LCF analysis (Table 2) showed that Cu was primarily associated with the adsorbed species on ferrihydrite (3–57%) and goethite (ND-59%), and sulfide bound Cu (CuS, 17–70%). Copper is also ready to bind with organic ligands present in the soil samples, which species is represented by the standard reference Cu-oxalate with a fitting range of ND-41%.

To investigate the forms of Cu uptake, Cu species in root samples were analyzed using XANES. The PCA analysis indicated that three components contributed to 93.4% of the samples spectra (Table S3), and all the standard references were appropriate for LCF analysis based on TT analysis (Table S4). The fitting results (Table 2) indicated that Cu was primarily complexed with organic ligands, including C/N ligand (histidine with 23–50% and alginate with ND-15%) and thiol-S ligand (glutathione with 8–56% and cysteine with ND-54%). In general, Cu binds with organic ligands as the key detoxification process in plant. The LCF analysis indicated that thiol-S like ligands (glutathione and cysteine) associated Cu(I) complex contributed to 51–67% in the root samples.

Iron species in the soil samples were analyzed using XANES technique after PCA/TT analysis (Fig. 2-I and Tables S5–6). The XANES LCF analysis indicated that ferrihydrite (58–100%) and goethite (ND-32%) were the main iron oxides in the collected soil samples (Table S7). Only a low amount of Fe-containing phyllosilicate minerals, including illite (9%) and olivine (2%) was observed for LQ2, suggesting significant weathering processes in the soil. In addition, a lot of Fe content in the soil should come from the irrigated wastewater, which usually precipitates as Fe (hydro) oxides in the irrigated soil. Ferrihydrite and goethite often contribute to large adsorption capacity for trace metals in soil, and can affect the geochemical behaviors of trace metals.

3.4. Spatial distribution and species of Cu in rice root section using μ-XRF and μ-XANES

In the paddy soil, Cu is desorbed from iron mineral surface by various organic ligands and inorganic chemicals before plant uptake. Therefore, to reveal the uptake procedures of Cu from soil to plant, especially for Cu spatial species in the specific area of root cross-section

Table 2
Copper species (%) in the soil samples (series of LQ and LX), rice root samples (series of LQR), and points of interest (POI) from μ-XRF map in Fig. 3 using linear combination fit analysis of Cu K-edge XANES (Fig. 1) and μ-XANES (Fig. 3). Cu-C/N ligand complexes include Cu-alginate and Cu-histidine, and Cu(I)-Thiol (S) includes Cu(I)-glutathione and Cu(I)-cysteine.

Sample	Cu-Fh	Cu-Gt	CuS	Cu-oxalate	Cu-C/N ligands	Cu(I)-thiol (S)	R-factor	Reduced χ^2
Soil samples								
LQ1	57	3	40				0.0019	0.0004
LQ2	3	32	25	39			0.0008	0.0006
LQ3	27	26	17	30			0.0006	0.0004
LQ4	20	27	38	15			0.0022	0.0005
LQ5	50	7	43				0.0008	0.0002
LQ6	47		53				0.0012	0.0002
LX1	18	12	70				0.0013	0.0003
LX2	21	13	66				0.0014	0.0003
LX3	20	16	64				0.0014	0.0003
LX4 non-rhi	38	21		41			0.0048	0.0012
LX4 rhi		59		41			0.0069	0.0004
Root samples								
LQR1					50	51	0.0084	0.0016
LQR2					32	67	0.0031	0.0006
LQR3					39	62	0.0032	0.0004
LQR4					43	58	0.0046	0.0009
LQR5					44	56	0.0195	0.0046
LQR6					34	66	0.0061	0.0013
POI-1					83	16	0.0310	0.0063
POI-2					66	34	0.0312	0.0084
POI-3					44	56	0.0062	0.0021
POI-4					35	65	0.0218	0.0034

R factor, goodness-of-fit parameter, $\Sigma(\chi_{data} - \chi_{fit})^2/\Sigma(\chi_{data})^2$; χ^2 represents the fitting quality of the XANES data.

region, coupling techniques of μ-XRF (Fig. 3-I) with μ-XANES (Fig. 3-II) were employed on rice root section.

The μ-XRF mapping showed that most of the absorbed Cu was mainly retained as a layer around the root outer layers, probably at the epidermis, with heterogeneous distribution (Fig. 3-I). The distribution of Cu around the root section for *Oryza sativa* was consistent with high abundance of Fe and other elements, showing a significantly linear correlation of Cu with Fe, Al, Mn, and other nutrient elements including K, Ca, P, and S (Figs. S1–2). The circular heterogeneous distribution of Fe around the root outer layers should be Fe plaque generated during rice culture (Carrasco-Gil et al., 2018). The consistent distribution of these elements among the root section suggested probably similar uptake of nutrients by plant. Besides the circular distribution of Cu around root surface, Cu was also shown around the internal cell layers of the rice root including endodermis and vascular cylinder, as identified by several hot spots of Cu (Fig. 3-I), suggesting successful uptake of Cu into root xylem and possible translocation to shoot.

From the μ-XRF region in the root cross-section, four points of interests (POIs 1–4) around the section were selected for μ-XANES analysis. The XANES LCF analysis indicated three primary Cu species in the root, including Cu(II)-alginate, Cu(I)-glutathione, and Cu(II)-histidine (Table 2). LCF analysis of POI1 and POI2 on the root surface indicated that Cu was mostly bound with C/N ligands like alginate (57–76%) and Cu(II)-histidine (7–9%), with a small amount of the other species including Cu(I)-glutathione (9–16%) and Cu(I)-cysteine (ND-25%). Furthermore, Cu adsorbed species on Fe minerals (ferrihydrite or goethite) was not observed on the root surface among the cross-sections in our study.

From root surface/epidermis to cortex and xylem, the proportion of alginate associated Cu species decreased gradually, and the proportion of Cu(I)-glutathione species increased accordingly in the root xylem. It is noted that the observed Cu(I)-thiol-S (glutathione and cysteine) complex species reached up to 16–34% on the root epidermis. In the root xylem, the existence of thiol-S containing ligands can reduce the bioavailability of Cu by forming Cu(I)-glutathione/cysteine as identified by increasing extent of the pre-edge peak at ~8984 eV (Fig. 3-II and Table 2).

4. Discussion

4.1. Copper contents in soil and rice plant

Dabaoshan mining activities have been in operation since 1960s (Zhou et al., 2007), which have induced significant contamination of heavy metals to nearby agricultural land owing to wastewater irrigation. As a result, the paddy soils showed elevated levels of Cu (Table 1) than the soil quality standard in China (50 mg-Cu/kg in GB 15618–1995) for safe agricultural use, posing potential risk to crops and human health. Besides, acidic wastewater used for irrigation also affected the soil pH condition. The lower pH of soil favors Cu desorption from soil minerals, especially for soil samples with pH below 5.5 (Antoniadis et al., 2017; Chaignon et al., 2009; Elliott et al., 1986; Martinez and Motto, 2000). Soil minerals and organic content largely affect the behavior of trace metals, and dissolved organic matter shows strong affinity with Cu and affects its mobility (Antoniadis et al., 2017; Cui et al., 2017; Krumins et al., 2015; Wu et al., 2010).

The normal average concentration of Cu in plant shoots/leaves is about 10 mg/kg dry weight, and > 20–30 mg/kg Cu may induce toxicity to plant with a wide range of physiological processes, such as pigment synthesis, photosynthesis, enzyme activity, cell wall metabolism, and finally resulting in defective growth (Adrees et al., 2015; Thounaojam et al., 2012; Yruela, 2009). Three of the thirteen rice samples showed higher Cu concentrations in shoot exceeding 20 mg/kg. Various soil factors may affect the Cu uptake process, and the concentrations of Cu in rice root shows a linear correlation with total Cu in soil ($r_s = 0.571$, $p < 0.05$), $CaCl_2$ extracted Cu ($r_s = 0.718$, $p < 0.01$), and rhizosphere-based chemicals extracted Cu ($r_s = 0.849$, $p < 0.01$) (Table S9), consistent with previous studies (Chaignon et al., 2009; Zhang et al., 2018; Zhao et al., 2014b; Zhao et al., 2011). Nevertheless, Cu content in shoot shows a linear correlation with Cu in $CaCl_2$ extraction ($r_s = 0.545$, $p < 0.05$) and rhizosphere-based extraction ($r_s = 0.516$, $p < 0.05$), but no correlation with total Cu in soil (Table S9). The more significant correlation of Cu in rice root and shoot with extracted Cu, especially by rhizosphere-based solution, indicated that the bioavailable Cu, rather the total concentration, is largely responsible for plant uptake. This is because that the bioavailable part of

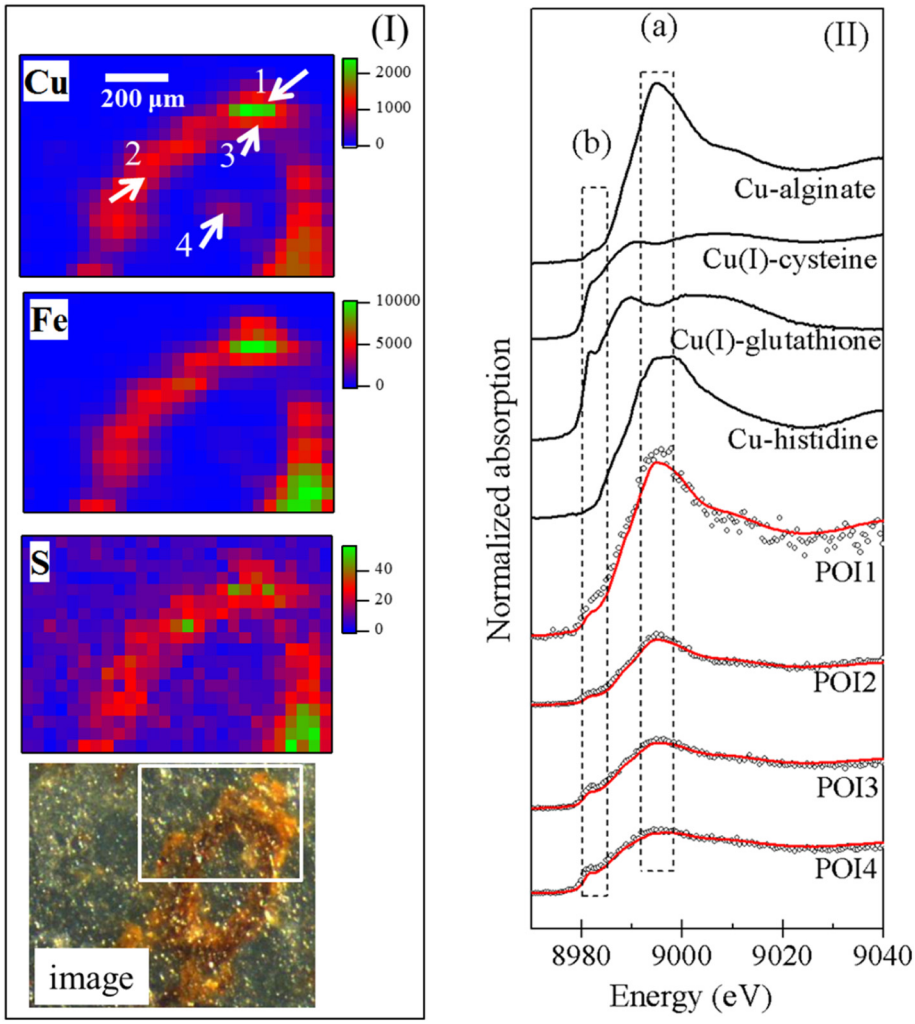

Fig. 3. (I) Light microscope and micro-X-ray fluorescence (μ-XRF) images around the root cross-section of *Oryza sativa*. Other maps of Al, Mn, Ca, K, P, and Si were shown in Fig. S1. White box in (image) shows where μ-XRF maps were obtained. (II) Corresponding μ-XANES of Cu species of the points of interest (POI 1–4) in the rice root section from panel I analyzed using linear combination fitting (Table 2).

Cu can be mostly affected by pH and organic matter in soil, especially the plant rhizosphere zone, which can affect Cu uptake by rice (Zhao et al., 2011). This may account for the relatively high concentration of Cu in rice grains identified in previous studies (Zhao et al., 2014b; Zhuang et al., 2009), and pose potential risk to human health.

4.2. Copper speciation in paddy soil

Considering source appointment, trace metals in the contaminated paddy soil came from the wastewater generated from Dabaoshan mining activities (Zhou et al., 2007; Zhou et al., 2015), and was usually adsorbed on iron oxides in soil with high retention capacity for trace metals (Cui et al., 2017; Yang et al., 2014), explaining the large part of adsorbed fraction of Cu (16–59%, Fig. 1 and Table 2). The organic matter associated Cu fraction like Cu-oxalate constitutes ND-41% of the total Cu in the paddy soil samples (Table 2), which may be partially taken up by rice (Fulda et al., 2013; Qin et al., 2004). In the paddy soil, rice often modulates nutrients (including Cu) uptake by secreting root exudate, which increases small organic ligands in the rhizosphere (Cui et al., 2017; Krumins et al., 2015; Qin et al., 2004; Tao et al., 2003), and thereby facilitates trace metal mobilization from both adsorbed and organic bound fractions.

In paddy soil, some sulfide complexed Cu(II) (CuS) was observed with ND-65% (Table 2). CuS was also reported in previous study (Pan et al., 2016) as free Cu(II) can be precipitated with reduced sulfide in paddy soil. Sulfide can be contributed by sulfate reducing bacteria in the paddy soil, especially under anaerobic conditions (Fulda et al., 2013; Lin et al., 2010), as high concentration of sulfate is drained from mining produced wastewater.

4.3. Spatial distribution and speciation of Cu and Fe from soil to rice root

Considering the spatial distribution of Cu in the root rhizosphere of rice, most of the absorbed Cu was retained as a layer around the root surface/rhizodermis identified by μ-XRF mapping (Fig. 3-I). The distribution of circular Cu around rice root is generally consistent with previous reports using other plant species like bamboo (exposing 100 mM Cu plus 1.1 mM Si in hydroponic conditions for 70 days) (Collin et al., 2014), cowpea (1.5 μM Cu in hydroponic condition for 24 h) (Kopittke et al., 2011), willow from contaminated floodplain soil (Zimmer et al., 2011), and *Phragmites australis* from an urban brownfield site (Feng et al., 2016). Several heavy metals also showed similar distribution pattern from root transversal section in other plant species, for instance, Pb in *Phragmites australis* from a brownfield site (Feng et al., 2016), Zn in *Euphorbia pithyusa* L. from a mine dump (Medas et al., 2015), Zn/Ni in willow from contaminated floodplain soil (Zimmer et al., 2011). Nevertheless, our rice sample from field contaminated site showed different Cu distribution from the laboratory

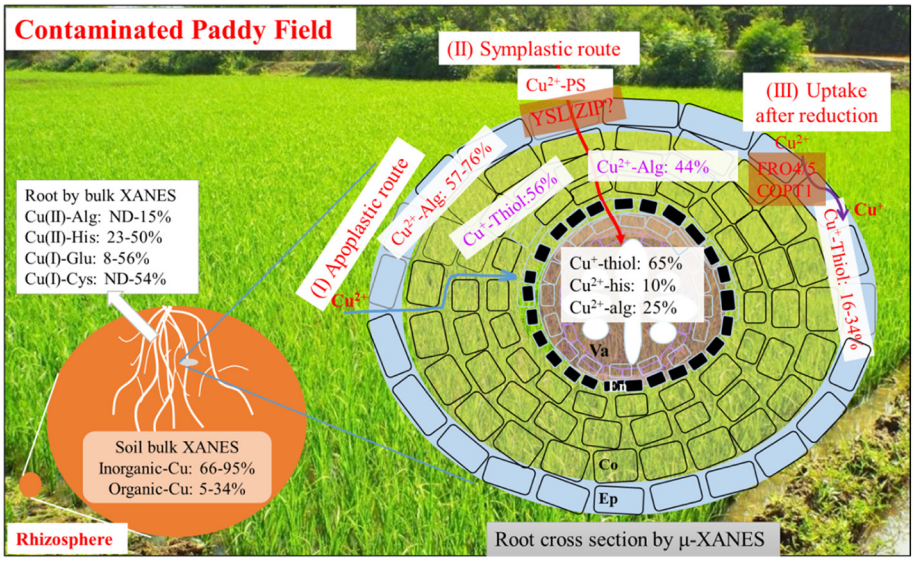

Fig. 4. Scheme of Cu mobilization/transformation in rhizosphere from contaminated paddy field soil and following uptake by rice root based on the finding in this study coupling with previous studies (Araki et al., 2011; Barberon et al., 2016; Bernal et al., 2012; Palmer and Guerinot, 2009; Yuan et al., 2011). Some abbreviations: Alg for alginate, Glu for glutathione, Cys for cysteine, His for histidine, Thiol-S ligand for glutathione and cysteine together, PS for phytosiderophore, YSL for yellow strip 1-like transporter, FRO4/5 for Fe or Cu reductase, and COPT1 for Cu transporter protein. Ep, epidermis; Co, cortex; En, Endodermis (Casparian strip); Va for vascular tissue. (For interpretation of the references to color in this figure legend, the reader is referred to the web version of this article.)

results using rice that Cu was mostly concentrated in the vascular tissues of *Oryza sativa* (50 μM Cu for 7 days) (Lu et al., 2017) and *Commelina communis* (100 μM for 15 days) (Shi et al., 2011), rather than in the rhizodermis or the outer cortex.

The difference of Cu distribution in root cross-section possibly resulted from different Cu concentration/species, exposure duration, and Cu contents in plant samples. From the current dataset, we hypothesize that in the field polluted site and hydroponic culture with high concentration of trace metals with a long period, plants developed various strategies such as secreting organic extrudes (Chaignon et al., 2009; Cui et al., 2017), sequestrating iron plaque on epidermis (Feng et al., 2018), and generating a biomineralization rim on root epidermis (Medas et al., 2015), to reduce the mobility and toxicity of the exposed toxins. For hydroponic solution with low concentrations (50–100 μM) in a short exposure period, plant may actively uptake Cu and Zn as nutrients to support plant growth (Feng et al., 2018). The accumulation of toxic metals within the cell wall on root surface is usually the first defense strategy for plant detoxification (Adrees et al., 2015; Colzi et al., 2012), which may efficiently limit the increase of Cu in root, and consequently in shoot and grains (Zhuang et al., 2009). The sequestered Cu was mostly bound with alginate (77%, Fig. 1-III and Table 2), as the cell wall structure bears abundant negatively charged carboxyl groups ready for Cu, Zn, and Pb retention (Hall, 2002; Jeon et al., 2002). Bulk XAS also indicated that continuous exposure of cowpea to 1.5 μM Cu from 6 to 24 h has changed the primary Cu complex from cysteine and histidine to polygalacturonic acid (Kopittke et al., 2011), suggesting the presence of more affinity sites in cell wall components for Cu.

Similar to Cu, the circular distribution of Fe around the rice root surface (Fig. 3) often generates Fe plaque on root surface by Fe(II) oxidation via rhizosphere oxidation (Fresno et al., 2016; Guo and Cutright, 2015). Iron plaque around the roots in both arid and paddy soil often sequesters trace metals and inhibits their translocation from root surface/epidermis to root endodermis/cortex (Cui et al., 2015b; Feng et al., 2016; Fresno et al., 2016). Similar association of Cu, Ni, and Zn with Fe around the plant root surface was found in previous studies (Feng et al., 2016; Ye et al., 1997). However, the consistent spatial distributions of trace metals with Fe do not necessarily confirm the chemical complexation between trace elements and Fe. In our study on the root surface, the adsorption complex of Cu with ferrihydrite or goethite was not found, indicating that the Fe plaque is not a dominant Cu sequestrator for rice. For Cd, another toxic trace metal, one study indicated that root tissue on the root surface rather than iron plaque contributes to Cd uptake in root and therefore inhibited Cd translocation to the aerial part of rice (Liu et al., 2007). Therefore, the interaction between trace metal and Fe plaque cannot be determined by the spatial distribution analysis alone as the rhizosphere niche is very complicated.

4.4. Implications for Cu uptake and transformation in rice plant

The uptake and transformation of Cu in plant is complex, depending on plant species, Cu concentrations and chemical species, and environmental conditions (Adrees et al., 2015; Printz et al., 2016; Zhao et al., 2014a). Excess free Cu ions can bring significant toxicity to plant, and therefore plant develops various defense systems by complexing Cu with many kinds of ligands, resulting in very little free ion within plant. Free cupric Cu(II) is often bound by oxygen in alginate or nitrogen in histidine like ligands with less mobility (Collin et al., 2014). Cu-alginate like structure is often not mobile as cell wall sequestered much Cu in detoxification process. However, Cu(II)-histidine like complex can be transported in xylem and translocated from root to shoot (Ryan et al., 2013). Another large portion of free Cu(II) is usually reduced to Cu(I) by thiol-S groups in metallothioneins and phytochelatins, including cysteine or glutathione forming stable S-bridged Cu(I) clusters, and, correspondingly, excess Cu can activate the functional enzymes for more synthesis of metallothioneins and phytochelatins (Cobbett and Goldsbrough, 2002; Polette et al., 2000). The stable Cu(I)-thiol (S) complex in plant tissues is considered as less toxic than free Cu (Collin et al., 2014; Polette et al., 2000; Ryan et al., 2013). The observation of Cu(I)-ligand species throughout roots and leaves suggested reductive detoxification of Cu(II) in appropriate plant tissues (Kopittke et al., 2011; Ryan et al., 2013). Furthermore, Cu(I)-thiol (S) complex can be transported to leaves during long-distance transport, as several Cu complexes with thiol (S) ligands, including glutathione and cysteine, have been separated from xylem saps (Wei et al., 2007; Yruela, 2009).

Direct in situ observation of the spatial distribution of Cu molecular species in rice root provided important information for elucidating Cu uptake and transformation. Based on current results and previous reports, a scheme is proposed for Cu accumulation fate in rice plant from the real contaminated paddy soil (Fig. 4). In the contaminated soil, the adsorbed species of Cu (Cu-ferrihydrite or Cu-goethite) is often mobilized as free Cu associated with organic ligands, which is often facilitated by root exudate as phytoavailable Cu. Then the phytoavailable Cu can be transported from soil solution to the rhizosphere during plant transpiration process (Tani and Barrington, 2005). During uptake in the root cross region (Fig. 4), the spatial distribution of Cu(II) (83% for POI1, Fig. 3 and Table 2) on the root surface suggested that high amount of Cu(II) was taken by root because soil bears Cu(II) as the

primary species (Fig. 1-II and Table 2). The large amount of C/N ligand complexed Cu(II) on the root surface and root internal portion are much less mobile than free Cu(II), because the negatively charged cell wall structure is the effective defense barrier of rice for metal retention (Printz et al., 2016), and therefore limited the translocation of Cu to rice shoot and grains.

Trace metals can be uptake and transported radially across the root cell layers through symplastic pathway, apoplastic pathway, and coupled transcellular pathway (Barberon et al., 2016; Doblas et al., 2017). The symplastic pathway is selective requiring trace metals to pass through identical cell membranes/transporters on epidermis, which critically affect Cu acquisition and transformation. During the plant uptake (Fig. 4), Cu(II) can be absorbed via YSL or ZIP membrane transporter (Araki et al., 2011; Palmer and Guerinot, 2009; Printz et al., 2016). Apoplastic route (Fig. 4-I) also contributes to Cu(II) uptake (Fu et al., 2015; Ranathunge et al., 2005), in which Cu often binds with root cell wall for detoxification or tolerance of excess Cu (Adrees et al., 2015; Colzi et al., 2012).

The reduction mechanism of Cu(II) to Cu(I) during uptake on root epidermis has not been elucidated yet, especially for the strategy II monocot plant including rice. Our study observed Cu(I) bound with thiol-S ligand (glutathione or cysteine) (16% for POI1, 59% for POI2, and 56% for POI3) on the root surface possibly on the root epidermis. Considering no observation of Cu(I) in the bulk and rhizosphere soil, this is the first direct observation of Cu(I) on root surface/epidermis, although Cu(I) was found widely in monocot plant bulk root like oat root (Ryan et al., 2013) and rice root (Lu et al., 2017) using bulk XAS technique which could not identify the exact location of Cu(I) among the root cross-section. The observation of large amount of Cu(I) on root epidermis may be caused by the reduction of Cu(II) via FRO4/FRO5 (Bernal et al., 2012), possibly forming complex of Cu(I)-thiol-S ligand with reduced toxicity (Collin et al., 2014; Polette et al., 2000). The related COPT/Ctr-type copper transporter-like gene family dominates the transport of Cu(I) in dicot root (*Arabidopsis thaliana*) (Bernal et al., 2012; Printz et al., 2016), and the gene family has been found in rice by Yuan et al. (2011). Therefore, a plant reduction process for Cu(II) may occur at the root epidermis during Cu uptake in rice, which was also evidenced by the lighter Cu isotopes (Jouvin et al., 2012). Nevertheless, this lighter Cu isotope fractionation result was not confirmed in oat roots (Ryan et al., 2013), probably because of various abiotic processes and uptake pathways of Cu on the root surface. The direct observation of Cu(I) with thiol-S ligands on the root epidermis for monocot species *Oryza sativa* using combined μ-XRF & μ-XANES provided another solid evidence for the previous hypothesis of reductive uptake of Cu.

In the root xylem during Cu transportation from root to shoot, thiol-S containing ligands in root can reduce the bioavailability of Cu by forming Cu(I)-glutathione as observed for POI4 in Fig. 3. The observed organic complex of Cu-histidine and Cu(I)-glutathione in the root vascular tissues for *Oryza sativa* may be transported to the aerial part (Ryan et al., 2013; Zhao et al., 2018). The primary Cu species including Cu(I)-glutathione (GSH), Cu(I)-cysteine and Cu(II)-histidine were also observed in roots of oat, rice, and tomato (Lu et al., 2017; Ryan et al., 2013; Sun et al., 2017). These Cu(II) reduction processes alleviated the toxicity and damage of Cu to some extent (Collin et al., 2014; Polette et al., 2000).

5. Conclusions

The current study investigated the change of Cu abundance and speciation from mining-contaminated paddy soil to rice root, focusing on the molecular fate of Cu in the rhizosphere system. Much high concentration of Cu was observed in rice root, which was largely affected by the bioavailable part of Cu in soil. Synchrotron based μ-XRF indicated that most Cu was sequestered in rice root surface and epidermis rather than xylem. Micro XANES techniques indicated that Cu was bound with C/N ligands, such as alginate and histidine on root surface. Thiol-S bound Cu(I) complex (Cu(I)-glutathione and Cu(I)-cysteine) was observed in the root xylem, representing the reductive detoxification of uptake Cu(II) by thiol-S ligands in rice. The transformation of Cu distribution and molecular species from soil to root surface and xylem shed lights on Cu uptake and transformation mechanisms in rice, and subsequently on food safety assessment. Further study on the selection of rice varieties that show high Cu detoxification ability and high Cu sequestration in root with low Cu uptake can be a possible remediation method to reduce the health risk from dietary Cu exposure in the mining-contaminated area.

Acknowledgments

The work was supported by Natural Science Foundation of China (NFSC 41603093), the Hong Kong RGC Collaborative Research Fund (RGC C7044-14G), and the National Basic Research Program of China (973 Program) 2014CB441101. The μ-XRF and μ-XANES results were acquired at BL15U1 beamline 15U at SSRF, and other XAS results were obtained at beamlines 01C1 and 16A1 at the National Synchrotron Radiation Research Center (NSRRC) in Taiwan. We acknowledge the kind help on providing some Cu reference XAS spectra from Prof. Jianjun Yang, Dr. Li-juan Sun, Prof. Ji-yan Shi, and Dr. Song-lin Wu.

Appendix A. Supplementary data

Supplementary data to this article can be found online at https://doi.org/10.1016/j.envint.2019.02.045.

References

Adamo, P., Agrelli, D., Zampella, M., 2018. Book. Belkin, H.E. and Lima, A. (Eds), Environmental Geochemistry (Second Edition), Elsevier, pp. 153–194.

Adrees, M., Ali, S., Rizwan, M., Ibrahim, M., Abbas, F., Farid, M., Zia-ur-Rehman, M., Irshad, M.K., Bharwana, S.A., 2015. The effect of excess copper on growth and physiology of important food crops: a review. Environ. Sci. Pollut. Res. 22 (11), 8148–8162.

Antoniadis, V., Levizou, E., Shaheen, S.M., Ok, Y.S., Sebastian, A., Baum, C., Prasad, M.N.V., Wenzel, W.W., Rinklebe, J., 2017. Trace elements in the soil-plant interface: phytoavailability, translocation, and phytoremediation—a review. Earth Sci. Rev. 171, 621–645.

Araki, R., Murata, J., Murata, Y., 2011. A novel barley yellow stripe 1-like transporter (HvYSL2) localized to the root endodermis transports metal-phytosiderophore complexes. Plant Cell Physiol. 52 (11), 1931–1940.

Barberon, M., Vermeer, Joop Engelbertus, De Bellis, D., Wang, P., Naseer, S., Andersen, Tonni G., Humbel, Bruno M., Nawrath, C., Takano, J., Salt, David E., Geldner, N., 2016. Adaptation of root function by nutrient-induced plasticity of endodermal differentiation. Cell 164 (3), 447–459.

Beiyuan, J., Awad, Y.M., Beckers, F., Tsang, D.C.W., Ok, Y.S., Rinklebe, J., 2017. Mobility and phytoavailability of As and Pb in a contaminated soil using pine sawdust biochar under systematic change of redox conditions. Chemosphere 178, 110–118.

Bernal, M., Casero, D., Singh, V., Wilson, G.T., Grande, A., Yang, H., Dodani, S.C., Pellegrini, M., Huijser, P., Connolly, E.L., Merchant, S.S., Krämer, U., 2012. Transcriptome sequencing identifies SPL7-regulated copper acquisition genes FRO_4/FRO_5 and the copper dependence of iron homeostasis in *Arabidopsis*. Plant Cell 24 (2), 738–761.

Cai, Q.-Y., Mo, C.-H., Li, Y.-H., Zeng, Q.-Y., Katsoyiannis, A., Wu, Q.-T., Férard, J.-F., 2007. Occurrence and assessment of polycyclic aromatic hydrocarbons in soils from vegetable fields of the Pearl River Delta, South China. Chemosphere 68 (1), 159–168.

Carrasco-Gil, S., Rodríguez-Menéndez, S., Fernández, B., Pereiro, R., de la Fuente, V., Hernandez-Apaolaza, L., 2018. Silicon induced Fe deficiency affects Fe, Mn, Cu and Zn distribution in rice (Oryza sativa L.) growth in calcareous conditions. Plant Physiol. Biochem. 125, 153–163.

Chaignon, V., Quesnoit, M., Hinsinger, P., 2009. Copper availability and bioavailability are controlled by rhizosphere pH in rape grown in an acidic Cu-contaminated soil. Environ. Pollut. 157 (12), 3363–3369.

Cobbett, C., Goldsbrough, P., 2002. Phytochelatins and metallothioneins: roles in heavy metal detoxification and homeostasis. Annu. Rev. Plant Biol. 53 (1), 159–182.

Collin, B., Doelsch, E., Keller, C., Cazevieille, P., Tella, M., Chaurand, P., Panfili, F., Hazemann, J.L., Meunier, J.D., 2014. Evidence of sulfur-bound reduced copper in bamboo exposed to high silicon and copper concentrations. Environ. Pollut. 187, 22–30.

Colzi, I., Arnetoli, M., Gallo, A., Doumett, S., Del Bubba, M., Pignattelli, S., Gabbrielli, R., Gonnelli, C., 2012. Copper tolerance strategies involving the root cell wall pectins in Silene paradoxa L. Environ. Exp. Bot. 78, 91–98.

ASTM Committee, 1998. Standard test method for particle-size analysis of soils, United States. D 422-63.

Cui, J.L., Shi, J.B., Jiang, G.B., Jing, C.Y., 2013. Arsenic levels and speciation from ingestion exposures to biomarkers in Shanxi, China: implications for human health. Environ. Sci. Technol. 47 (10), 5419–5424.
Cui, J.L., Jing, C.Y., Che, D.S., Zhang, J.F., Duan, S.X., 2015a. Groundwater arsenic removal by coagulation using ferric(III) sulfate and polyferric sulfate: a comparative and mechanistic study. J. Environ. Sci. 32, 42–53.
Cui, J.L., Luo, C.L., Tang, C.W.Y., Chan, T.S., Li, X.D., 2017. Speciation and leaching of trace metal contaminants from e-waste contaminated soils. J. Hazard. Mater. 329, 150–158.
Cui, J.L., Zhao, Y.P., Li, J.S., Beiyuan, J.Z., Tsang, D.C.W., Poon, C.S., Chan, T.S., Wang, W.X., Li, X.D., 2018. Speciation, mobilization, and bioaccessibility of arsenic in geogenic soil profile from Hong Kong. Environ. Pollut. 232, 375–384.
Cui, J.L., Zhao, Y.P., Chan, T.S., Zhang, L., Tsang, D.C.W., Li, X.D., 2019. Spatial Distribution and Molecular Speciation of Copper in Indigenous Plants From Contaminated Mine Sites: Implication for Phytostabilization. (Submitted).
Cui, X.D., Wang, Y.J., Hockmann, K., Zhou, D.M., 2015b. Effect of iron plaque on antimony uptake by rice (Oryza sativa L.). Environ. Pollut. 204, 133–140.
Doblas, V.G., Geldner, N., Barberon, M., 2017. The endodermis, a tightly controlled barrier for nutrients. Curr. Opin. Plant Biol. 39, 136–143.
Elliott, H.A., Liberati, M.R., Huang, C.P., 1986. Competitive adsorption of heavy metals by soils. J. Environ. Qual. 15 (3), 214–219.
Feng, M.H., Shan, X.Q., Zhang, S., Wen, B., 2005. A comparison of the rhizosphere-based method with DTPA, EDTA, $CaCl_2$, and $NaNO_3$ extraction methods for prediction of bioavailability of metals in soil to barley. Environ. Pollut. 137 (2), 231–240.
Feng, H., Qian, Y., Gallagher, F.J., Zhang, W.G., Yu, L.Z., Liu, C.J., Jones, K.W., Tappero, R., 2016. Synchrotron micro-scale measurement of metal distributions in *Phragmites australis* and *Typha latifolia* root tissue from an urban brownfield site. J. Environ. Sci. 41, 172–182.
Feng, H., Qian, Y., Cochran, J.K., Zhu, Q., Heilbrun, C., Li, L., Hu, W., Yan, H., Huang, X., Ge, M., Nazareski, E., Chu, Y.S., Yoo, S., Zhang, X., Liu, C.-J., 2018. Seasonal differences in trace element concentrations and distribution in Spartina alterniflora root tissue. Chemosphere 204, 359–370.
Fresno, T., Peñalosa, J.M., Santner, J., Puschenreiter, M., Prohaska, T., Moreno-Jiménez, E., 2016. Iron plaque formed under aerobic conditions efficiently immobilizes arsenic in Lupinus albus L roots. Environ. Pollut. 216, 215–222.
Fu, Y.Z., Lei, W.R., Shen, Z.G., Luo, C.L., 2015. Permeability of plant young root endodermis to Cu ions and Cu-citrate complexes in corn and soybean. Int. J. Phytoremediation 17 (9), 822–834.
Fulda, B., Voegelin, A., Ehlert, K., Kretzschmar, R., 2013. Redox transformation, solid phase speciation and solution dynamics of copper during soil reduction and reoxidation as affected by sulfate availability. Geochim. Cosmochim. Acta 123, 385–402.
Guo, L., Cutright, T.J., 2015. Effect of citric acid and bacteria on metal uptake in reeds grown in a synthetic acid mine drainage solution. J. Environ. Manag. 150, 235–242.
Hall, J.L., 2002. Cellular mechanisms for heavy metal detoxification and tolerance. J. Exp. Bot. 53 (366), 1–11.
Hansel, C.M., Fendorf, S., Sutton, S., Newville, M., 2001. Characterization of Fe plaque and associated metals on the roots of mine-waste impacted aquatic plants. Environ. Sci. Technol. 35 (19), 3863–3868.
Jeon, C., Park, J.Y., Yoo, Y.J., 2002. Characteristics of metal removal using carboxylated alginic acid. Water Res. 36 (7), 1814–1824.
Jouvin, D., Weiss, D.J., Mason, T.F.M., Bravin, M.N., Louvat, P., Zhao, F., Ferec, F., Hinsinger, P., Benedetti, M.F., 2012. Stable isotopes of Cu and Zn in higher plants: evidence for Cu reduction at the root surface and two conceptual models for isotopic fractionation processes. Environ. Sci. Technol. 46 (5), 2652–2660.
Kau, L.S., Spira-Solomon, D.J., Penner-Hahn, J.E., Hodgson, K.O., Solomon, E.I., 1987. X-ray absorption edge determination of the oxidation state and coordination number of copper. Application to the type 3 site in Rhus vernicifera laccase and its reaction with oxygen. J. Am. Chem. Soc. 109 (21), 6433–6442.
Kopittke, P.M., Menzies, N.W., de Jonge, M.D., McKenna, B.A., Donner, E., Webb, R.I., Paterson, D.J., Howard, D.L., Ryan, C.G., Glover, C.J., Scheckel, K.G., Lombi, E., 2011. In situ distribution and speciation of toxic copper, nickel, and zinc in hydrated roots of cowpea. Plant Physiol. 156 (2), 663–673.
Kopittke, P.M., Wang, P., Lombi, E., Donner, E., 2017. Synchrotron-based X-ray approaches for examining toxic trace metal(loid)s in soil–plant systems. J. Environ. Qual. 46, 1175–1189.
Krumins, J.A., Goodey, N.M., Gallagher, F., 2015. Plant-soil interactions in metal contaminated soils. Soil Biol. Biochem. 80, 224–231.
Li, X.D., Poon, C.-S., Liu, P.S., 2001. Heavy metal contamination of urban soils and street dusts in Hong Kong. Appl. Geochem. 16 (11), 1361–1368.
Lin, H., Shi, J., Wu, B., Yang, J., Chen, Y., Zhao, Y., Hu, T., 2010. Speciation and biochemical transformations of sulfur and copper in rice rhizosphere and bulk soil—XANES evidence of sulfur and copper associations, pp. In: 69–71, Springer. Berlin Heidelberg, Berlin, Heidelberg.
Liu, H.J., Zhang, J.L., Zhang, F.S., 2007. Role of iron plaque in Cd uptake by and translocation within rice (Oryza sativa L.) seedlings grown in solution culture. Environ. Exp. Bot. 59 (3), 314–320.
Lu, Y., Song, S., Wang, R., Liu, Z., Meng, J., Sweetman, A.J., Jenkins, A., Ferrier, R.C., Li, H., Luo, W., Wang, T., 2015. Impacts of soil and water pollution on food safety and health risks in China. Environ. Int. 77, 5–15.
Lu, L.L., Xie, R.H., Liu, T., Wang, H.X., Hou, D.D., Du, Y.H., He, Z.L., Yang, X.E., Sun, H., Tian, S.K., 2017. Spatial imaging and speciation of Cu in rice (Oryza sativa L.) roots using synchrotron-based X-ray microfluorescence and X-ray absorption spectroscopy. Chemosphere 175, 356–364.
Manceau, A., Simionovici, A., Lanson, M., Perrin, J., Tucoulou, R., Bohic, S., Fakra, S.C., Marcus, M.A., Bedell, J.-P., Nagy, K.L., 2013. Thlaspi arvense binds Cu(II) as a bis-(l-histidinato) complex on root cell walls in an urban ecosystem. Metallomics 5 (12), 1674–1684.
Martinez, C.E., Motto, H.L., 2000. Solubility of lead, zinc and copper added to mineral soils. Environ. Pollut. 107 (1), 153–158.
McBride, M.B., Cai, M., 2016. Copper and zinc aging in soils for a decade: changes in metal extractability and phytotoxicity. Environ. Chem. 13 (1), 160–167.
Medas, D., De Giudici, G., Casu, M.A., Musu, E., Gianoncelli, A., Iadecola, A., Meneghini, C., Tamburini, E., Sprocati, A.R., Turnau, K., Lattanzi, P., 2015. Microscopic processes ruling the bioavailability of Zn to roots of euphorbia pithyusa L. pioneer plant. Environ. Sci. Technol. 49 (3), 1400–1408.
Mijovilovich, A., Leitenmaier, B., Meyer-Klaucke, W., Kroneck, P.M.H., Gotz, B., Kupper, H., 2009. Complexation and toxicity of copper in higher plants. II. Different mechanisms for copper versus cadmium detoxification in the copper-sensitive cadmium/zinc hyperaccumulator Thlaspi caerulescens (Ganges ecotype). Plant Physiol. 151 (2), 715–731.
Palmer, C.M., Guerinot, M.L., 2009. Facing the challenges of Cu, Fe and Zn homeostasis in plants. Nat. Chem. Biol. 5 (5), 333–340.
Pan, Y., Bonten, L.T.C., Koopmans, G.F., Song, J., Luo, Y., Temminghoff, E.J.M., Comans, R.N.J., 2016. Solubility of trace metals in two contaminated paddy soils exposed to alternating flooding and drainage. Geoderma 261, 59–69.
Polette, L.A., Gardea-Torresdey, J.L., Chianelli, R.R., George, G.N., Pickering, I.J., Arenas, J., 2000. XAS and microscopy studies of the uptake and bio-transformation of copper in Larrea tridentata (creosote bush). Microchem. J. 65 (3), 227–236.
Printz, B., Lutts, S., Hausman, J.F., Sergeants, K., 2016. Copper trafficking in plants and its implication on cell wall dynamics. Front. Plant Sci. 7.
Qin, F., Shan, X.-Q., Wei, B., 2004. Effects of low-molecular-weight organic acids and residence time on desorption of Cu, Cd, and Pb from soils. Chemosphere 57 (4), 253–263.
Ranathunge, K., Steudle, E., Lafitte, R., 2005. A new precipitation technique provides evidence for the permeability of Casparian bands to ions in young roots of corn (Zea mays L.) and rice (Oryza sativa L.). Plant Cell Environ. 28 (11), 1450–1462.
Rinklebe, J., Shaheen, S.M., Yu, K., 2016. Release of As, Ba, Cd, Cu, Pb, and Sr under predefinite redox conditions in different rice paddy soils originating from the U.S.A. and Asia. Geoderma 270, 21–32.
Ryan, B.M., Kirby, J.K., Degryse, F., Harris, H., McLaughlin, M.J., Scheiderich, K., 2013. Copper speciation and isotopic fractionation in plants: uptake and translocation mechanisms. New Phytol. 199 (2), 367–378.
Shi, J.Y., Yuan, X.F., Chen, X.C., Wu, B., Huang, Y.Y., Chen, Y.X., 2011. Copper uptake and its effect on metal distribution in root growth zones of Commelina communis revealed by SRXRF. Biol. Trace Elem. Res. 141 (1), 294–304.
Shi, J.Y., Sun, L.J., Peng, C., Xu, C., Wang, Y.P., Chen, X.C., Lin, H.R., Yang, J.J., Liu, T.T., Chen, Y.X., 2018. In: Luo, Y., Tu, C. (Eds.), Twenty Years of Research and Development on Soil Pollution and Remediation in China. Springer Singapore, Singapore, pp. 151–164.
Sun, L., Yang, J., Fang, H., Xu, C., Peng, C., Huang, H., Lu, L., Duan, D., Zhang, X., Shi, J., 2017. Mechanism study of sulfur fertilization mediating copper translocation and biotransformation in rice (Oryza sativa L.) plants. Environ. Pollut. 226, 426–434.
Tani, F.H., Barrington, S., 2005. Zinc and copper uptake by plants under two transpiration rates. Part I. Wheat (Triticum aestivum L.). Environ. Pollut. 138 (3), 538–547.
Tao, S., Chen, Y.J., Xu, F.L., Cao, J., Li, B.G., 2003. Changes of copper speciation in maize rhizosphere soil. Environ. Pollut. 122 (3), 447–454.
Thounaojam, T.C., Panda, P., Mazumdar, P., Kumar, D., Sharma, G.D., Sahoo, L., Sanjib, P., 2012. Excess copper induced oxidative stress and response of antioxidants in rice. Plant Physiol. Biochem. 53, 33–39.
Tóth, G., Hermann, T., Da Silva, M.R., Montanarella, L., 2016. Heavy metals in agricultural soils of the European Union with implications for food safety. Environ. Int. 88, 299–309.
Wei, Z.G., Wong, J.W.C., Zhao, H.Y., Zhang, H.J., Li, H.X., Hu, F., 2007. Separation and determination of heavy metals associated with low molecular weight chelators in xylem saps of Indian Mustard (Brassica juncea) by size exclusion chromatography and atomic absorption spectrometry. Biol. Trace Elem. Res. 118 (2), 146–158.
Wu, C.F., Luo, Y.M., Zhang, L.M., 2010. Variability of copper availability in paddy fields in relation to selected soil properties in southeast China. Geoderma 156 (3–4), 200–206.
Xu, C., Chen, X., Duan, D., Peng, C., Le, T., Shi, J., 2015. Effect of heavy-metal-resistant bacteria on enhanced metal uptake and translocation of the Cu-tolerant plant, Elsholtzia splendens. Environ. Sci. Pollut. Res. 22 (7), 5070–5081.
Yang, J.J., Liu, J., Dynes, J.J., Peak, D., Regier, T., Wang, J., Zhu, S.H., Shi, J.Y., Tse, J.S., 2014. Speciation and distribution of copper in a mining soil using multiple synchrotron-based bulk and microscopic techniques. Environ. Sci. Pollut. Res. 21 (4), 2943–2954.
Ye, Z.H., Baker, A.J.M., Wong, M.H., Willis, A.J., 1997. Copper and nickel uptake, accumulation and tolerance in Typha latifolia with and without iron plaque on the root surface. New Phytol. 136 (3), 481–488.
Yruela, I., 2009. Copper in plants: acquisition, transport and interactions. Funct. Plant Biol. 36 (5), 409–430.
Yuan, M., Li, X.H., Xiao, J.H., Wang, S.P., 2011. Molecular and functional analyses of COPT/Ctr-type copper transporter-like gene family in rice. BMC Plant Biol. 11.
Zeng, F., Cui, K., Xie, Z., Wu, L., Liu, M., Sun, G., Lin, Y., Luo, D., Zeng, Z., 2008. Phthalate esters (PAEs): emerging organic contaminants in agricultural soils in peri-urban areas around Guangzhou, China. Environ. Pollut. 156 (2), 425–434.
Zhang, J., Li, H., Zhou, Y., Dou, L., Cai, L., Mo, L., You, J., 2018. Bioavailability and soil-to-crop transfer of heavy metals in farmland soils: a case study in the Pearl River Delta, South China. Environ. Pollut. 235, 710–719.
Zhao, K., Liu, X., Zhang, W., Xu, J., Wang, F., 2011. Spatial dependence and bioavailability of metal fractions in paddy fields on metal concentrations in rice grain at a regional scale. J. Soils Sediments 11 (7), 1165.

Zhao, F.J., Moore, K.L., Lombi, E., Zhu, Y.G., 2014a. Imaging element distribution and speciation in plant cells. Trends Plant Sci. 19 (3), 183–192.
Zhao, K., Fu, W., Liu, X., Huang, D., Zhang, C., Ye, Z., Xu, J., 2014b. Spatial variations of concentrations of copper and its speciation in the soil-rice system in Wenling of southeastern China. Environ. Sci. Pollut. Res. 21 (11), 7165–7176.
Zhao, Y.P., Cui, J.L., Chan, T.S., Dong, J.C., Chen, D.L., Li, X.D., 2018. Role of chelant on Cu distribution and speciation in Lolium multiflorum by synchrotron techniques. Sci. Total Environ. 621, 772–781.
Zhou, J.M., Dang, Z., Cai, M.F., Liu, C.Q., 2007. Soil heavy metal pollution around the Dabaoshan Mine, Guangdong Province, China. Pedosphere 17 (5), 588–594.
Zhou, M., Liao, B., Shu, W.S., Yang, B., Lan, C.Y., 2015. Pollution assessment and potential sources of heavy metals in agricultural soils around four Pb/Zn mines of Shaoguan city, China. Soil Sediment Contam. 24 (1), 76–89.
Zhuang, P., McBride, M.B., Xia, H., Li, N., Li, Z., 2009. Health risk from heavy metals via consumption of food crops in the vicinity of Dabaoshan mine, South China. Sci. Total Environ. 407 (5), 1551–1561.
Zimmer, D., Kruse, J., Baum, C., Borca, C., Laue, M., Hause, G., Meissner, R., Leinweber, P., 2011. Spatial distribution of arsenic and heavy metals in willow roots from a contaminated floodplain soil measured by X-ray fluorescence spectroscopy. Sci. Total Environ. 409 (19), 4094–4100.